

EVALUATION OF STEEL FRAME STRUCTURES WITH THE RESPONSE OF SEISMIC ISOLATORS

Mohammad BEYKZADE^{1*}, Alireza BAGHCHESARAEI², Omid Reza
BAGHCHESARAEI²,

¹ Department of Civil Engineering, Kharazmi University, Tehran, Iran

² Centre for Infrastructure Engineering, Western Sydney University, Sydney, Australia

Abstract

As science keeps evolving over time, new solutions are being put forward for reducing structural damage. One such solution is the use of seismic isolation systems. Seismic isolation systems reduce the response of structures to the force of earthquakes by reducing the input (force) acceleration when the natural period of the structure increases. Therefore, the use of seismic isolation systems is recommended in the analysis of diverse structures. This study was carried out on seismically isolated buildings with 8, 10, and 12 regular steel floors, modeled by a non-linear isolator in two-, or three-second periods. The differences in data and the responses of the buildings were compared with fixed-base buildings with 8, 10, and 12 floors.

Keywords: seismic isolation system, dynamic analysis, seismic isolator, earthquake engineering, steel building

1. INTRODUCTION

In 1982, the Malaysian Rubber Manufacturers Research Institute, a British company, invented a natural rubber compound which, with its intrinsic damping properties, did not require the use of damper components inside it. The intake of this compound is due to the addition of a very fine carbon black, Yarzins oils, and

¹ Corresponding author: Department of Civil Engineering, Kharazmi University, Tehran, Iran, e-mail: M.Beykzade@gmail.com

other special fillers. Damping can achieve a shear strain from 100% to 10-20%. The use of a high damping rubber bearing for the seismic seclusion of structures has turned out to be a very effective strategy for providing security from tremor harm ([4], [16]).

High damping rubber bearings stand out amongst the most frequently utilized disengagement frameworks for structures since the mechanical qualities of their various orientations may depend largely on the mixes used as part of a high damping elastic [10].

Nowadays, performance tests are required to affirm that bearing qualities are roughly equivalent to the plan parameters and that they fulfill the requirements of the plan. Unlike different sorts of orientation, for example, lead-elastic heading ([7], [8]), few examination models are now readily accessible [15] for investigating the history of high damping elastic orientation due to their complex mechanical qualities. Modern methods of construction are focused on better products that aim to improve business efficiency, quality, customer satisfaction, environmental performance, sustainability, and the predictability of delivery timescales ([2], [5]).

Space plays a vital role in architecture. People have always lived between many spaces and their existence is related to the being of these spaces ([3], [6]). Seismic isolation is favored over more traditional strategies, which depend mostly on fortifying auxiliary segments. Isolation techniques lessen the quake powers transmitted to the structure, which eliminates permanent harm to the structure itself, thereby securing substance and auxiliary components.

Although the basic principles of seismic isolation are obvious and known for centuries, structures that have been constructed accordingly cannot be found in large numbers [1, 11]. The common approach in the study of seismically isolated structures is to ignore the effects of the flexibility of the superstructure in minor and major seismic responses. With regard to the fact that the flexibility of the seismically isolated structure is mainly concentrated at the level of the isolation system, the superstructure behaves like a rigid body being affected by the earthquake [12, 18].

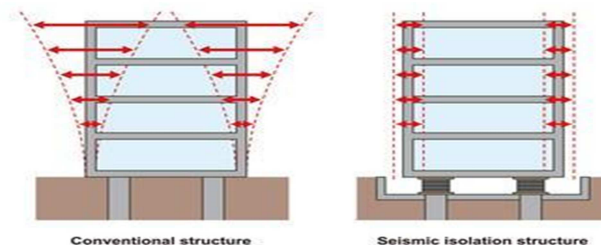


Fig. 1. Response of Conventional Structures and Base Isolated Structures to Earthquakes [17]

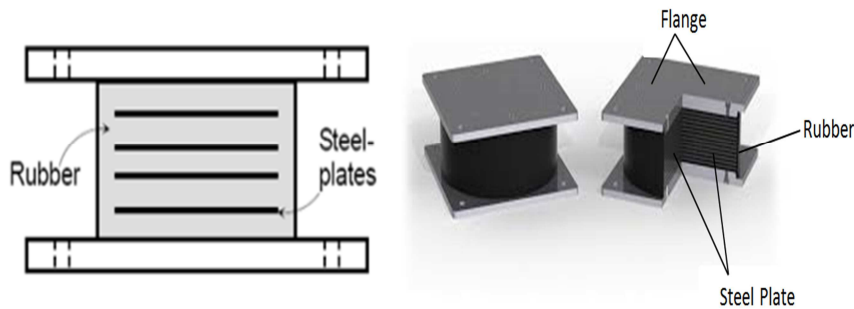


Fig. 2. Base isolation [9]

The research hypotheses are as follows:

1. Three types of 8, 10, and 12-floor structures are modeled in 3D.
2. Superstructures are regular.
3. The effects of soil and structure interaction are not considered.
4. The structures are identical in terms of the number of spans and the width of the frame's span.

The major objective of this research was to provide a simple, low-cost, and at the same time adequately accurate strategy for modeling and analyzing seismic isolators.

In addition, other objectives include:

1. Obtaining information on a structure with seismic isolation using a basic periodic seismic isolation system.
2. Determining the difference between the use of a fixed base structure and a non-linear isolation system.
3. Determining the acceleration change of the highest floor and the total drift of the building according to the change in height.

2. MATHEMATICAL MODELING

2.1. Superstructure

This research was carried out on buildings with 8, 10, and 12 floors with two forms of fixed base and seismic isolator. Each of the buildings was modeled in 3D and had a seismic isolator on the non-linear elastomeric isolation system with two periods of 2 and 3 seconds, respectively. Modular buildings have European steel sections. All columns have H400*237 sections while the beams have IPE180 sections. In the utilized structural modeling, the structural plan is in dimensions of 20 x 20, so that it consists of 4 openings with a length of 5 meters and the height of each floor is 3 meters. The modeling of floor diaphragms was

rigid with 3 degrees of rotational freedom in the x and y direction and thickness of 20 cm. All floors have dead and live loads of 4900 Nm/m² and 1960 Nm/m², and 2940 and 980 Nm/m², respectively. The total weight (W) of the 8-, 10-, and 12-floor models was 42241.71 kN, 51929.12 kN, and 61616.52 kN, respectively. According to the modal analysis using Sap 2000 software, the period of the 8, 10, and 12-floor fixed-base buildings was 0.96, 1.21, and 1.46 seconds, respectively.

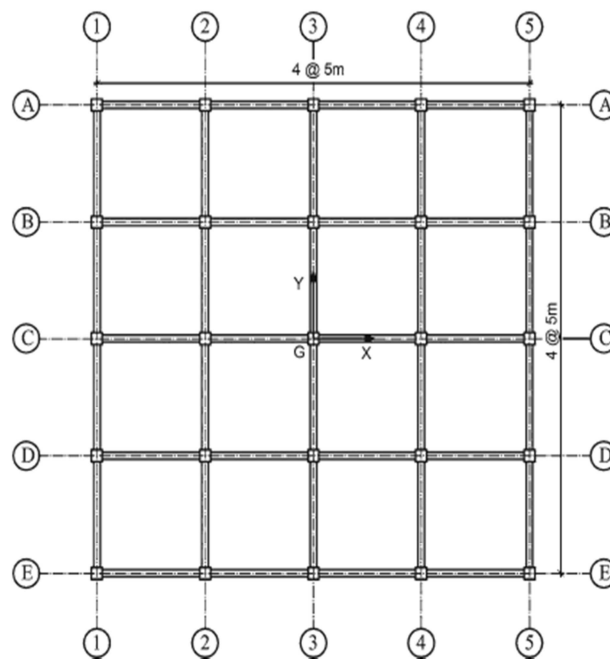


Fig. 3. Modeled Building Plan

2.2. Seismic Isolation

Non-linear isolation systems usually include dissipating rubber sheets exhibiting hysteresis and non-linear behavior. The relationship between force F and displacement D for the isolation system is shown in Fig. 4., where F_y = equals force yield, D_y = equals yield displacement, Q = characteristic force, K_1 = initial hardness, and K_2 = secondary hardness of the non-linear isolation system. The period of the non-linear isolation system is obtained as follows [14]:

$$T_o = 2\pi \sqrt{\frac{W}{K_2 g}} \quad (2.1)$$

Given that the period of the system (T_0) is 2 and 3 seconds, the K_2 value was obtained from the above formula. The stiffness ratio $\alpha = 0.1$ was used to obtain K_1 from the equation $\alpha = K_2/K_1$. The value of the characteristic force Q was obtained from the formula below [18]:

$$Q = (K_1 - K_2)D_y \quad (2.2)$$

Where D_y is the system yield limit and $D_y = 5\text{mm}$ for the period $T = 2\text{s}$; for the value and period $T = 3\text{s}$, $D_y = 10\text{mm}$ and the Q/W ratio is between 4-5%. All the above data are presented in Table 1.

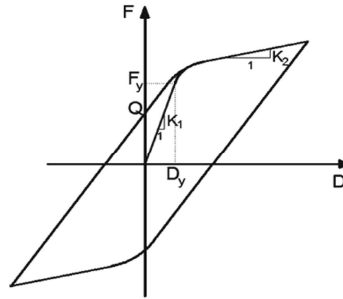


Fig. 4. Displacement-force behavior of non-linear isolation system [13]

Table 1. Non-linear Isolation System Specifications (HDRB NON-LINEAR ISOLATOR) ((A), $T_0=2\text{s}$ and (B), $T_0=3\text{s}$)

Number of Story	Non-linear Isolation System						
	$T_0=2\text{s}$						
A	W(kN)	$K_1(\text{kN/M})$	$K_2(\text{kN/M})$	$D_y(\text{mm})$	$F_y(\text{kN})$	Q(kN)	Q/W(%)
8	42241	424553	42455	5	2123	1910	4.52
10	51929	521917	52191	5	2609	2348	4.52
12	61616	619280	61928	5	3096	2786	4.52

Number of Story	Non-linear Isolation System`						
	$T_0=3\text{s}$						
B	W(kN)	$K_1(\text{kN/M})$	$K_2(\text{kN/M})$	$D_y(\text{mm})$	$F_y(\text{kN})$	Q(kN)	Q/W(%)
8	42241	188690	18869	10	1886	1698	4.02
10	51929	231963	23196	10	2319	2087	4.02
12	61616	275235	27523	10	2752	2477	4.02

In this analysis, an HDRB isolator is used. Due to the HDRB rubber isolator's disks, the performance increases over time as well as offering faster design time and lower cost of application. The movement of the structure equipped with an

elastomeric separation system is very slow and its oscillation period is long, the result of which is its movement is many times calmer and softer, so no serious damage is done to the structure.

Separation modeling is performed using SAP software which contains a member that can model the non-linearity of an elastomeric separator. Therefore, the isolator rubber element is used to model the separators in each of the models with seismic isolators under each of the 25 columns, according to weight, number of floors (height), and period.

2.3. Non-linear Dynamic Analysis

In the past, finite element analysis was purely an analytical tool but it has now entered the practical world of engineering design. Computer software with the ability to analyze is equipped with a finite element method, and design engineers widely use the finite element method in their design. Recently, most of the analytical software used by engineers has also been equipped with linear analysis. Linear analysis provides an acceptable approximation of the actual properties and behavior of most engineering problems, but in some non-linear cases, greater challenges arise and non-linear analysis can lead to serious design errors. Historically, engineers have been reluctant to use non-linear analysis due to the complex formulae and long-time span required to solve non-linear problems. But today, due to the existence of software with non-linear analysis capabilities, this approach has evolved with the use of limited components with an easy user interface. In addition, advanced problem-solving methods and powerful computers have greatly reduced problem-solving time. Over the past decade, engineers have considered the finite element method as a valuable, yet inaccessible design method. Today, design engineers are fully aware of the benefits of non-linear analysis using finite element methods and its use in design.

In this research, the type of structural analysis used is non-linear dynamics (time history analysis). The time history analysis method is the most accurate method of applying earthquake loads (due to ground accelerations) to the structure. To calculate the structural response in this scenario, historical analysis is used when referencing the ground motion records of previous earthquakes, and good information is obtained from poor land acceleration records as well as referring to 5 significant earthquakes that have occurred throughout history.

SAP 2000 software (Computers and Structures Inc.) was used on a time-based modal integral method through which the eigenvalues and eigenvectors necessary for dynamic analysis of buildings were analyzed.

3. EARTHQUAKE RECORD INFORMATION

Seismic data was first loaded from the site of the Pacific Earthquake Engineering Research Center (PEER) (Table 2) and data with a return period of 475 years was populated into the Seismosignal software so the desired earthquake acceleration was achieved. The stronger components of the records scaled to 9.81 (1g). Modal damping of 10% and a time step of 0.01 seconds are applied in the X-axis, while other components are applied in the Y-axis.

Table 2. Non-linear seismic parameters

Earthquake	Date	Station	Component	PGA(g)
Imperial valley	19/05/1940	El Centro	ELC180	0.280
Kocaeli	17/08/1999	16 LGPC	YPT150	0.321
Loma Prieta	18/10/1989	Yarımca	LPG090	0.607

4. DISCUSSION

4.1. Preface

Three types of 8-, 10-, and 12-floor buildings modeled with a fixed base, and a seismic isolator with a period of 2 and 3 seconds and three earthquakes, were applied to obtain basic acceleration information, acceleration of the highest floor, the base displacement, and total drift.

We aimed to demonstrate the ability and benefits of using a seismic isolator over a fixed and rigid support building, and it has also been well documented that an isolator reduces the response of seismic side forces and is expected to protect the structure with major energy diversion and absorption.

The mathematical model used in the SAP software shows the answers as follows:

Figures 5-13 show the response of the 8-story rigid support as well as the structure with the HDRB seismic isolator with 2 and 3 magnitude periods. Figures 14-22 show the modeling response of a 10-story building fixed support with a seismic isolator at $T = 2.3$ seconds. Finally, Figures 23-31 show the difference in the response of a structure with a seismic isolator versus the locked structure against earthquake forces. The contribution of this article to previous literature is that it defines the two parameters A, B, which are in sections 4.2 and 4.3, so that by fully examining the seismic response, the highest drift rate and peak floor acceleration can be obtained due to the increase in structural height ratio (4.2). In general, we obtained the response values variation coefficient from the locked structure to the seismic isolator structure, with the application of the lateral earthquake force (Section 4.3).

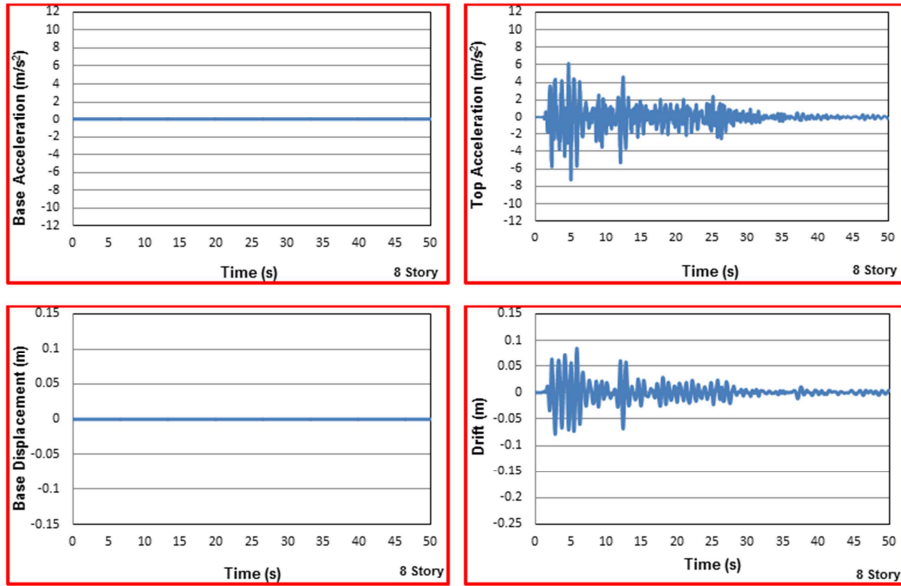


Fig. 5. Base acceleration and acceleration of the highest floor, base displacement and total drift of the 8-story fixed-base building under the Imperial Valley earthquake

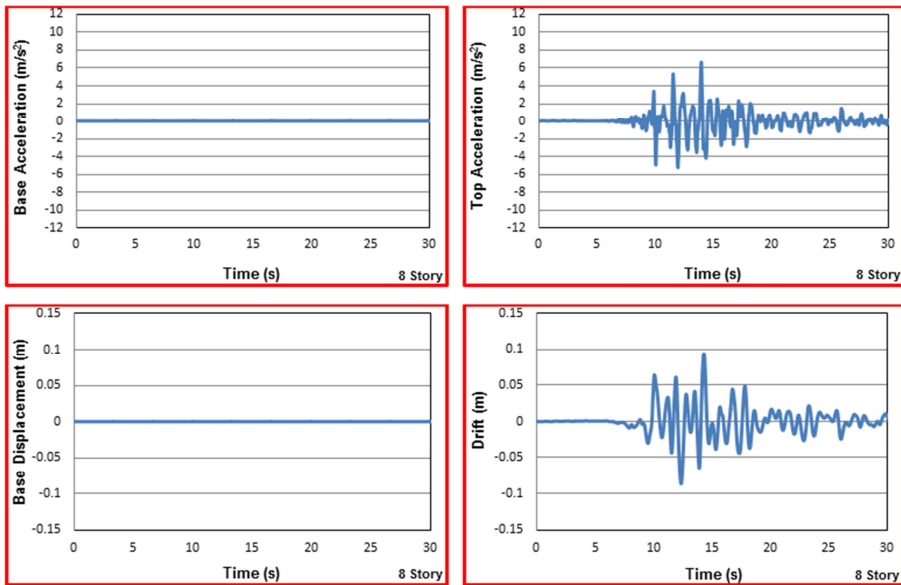


Fig. 6. Base acceleration and acceleration of the highest floor, base displacement and total drift of the 8-story fixed-base building under the Kocaeli (Izmit) earthquake

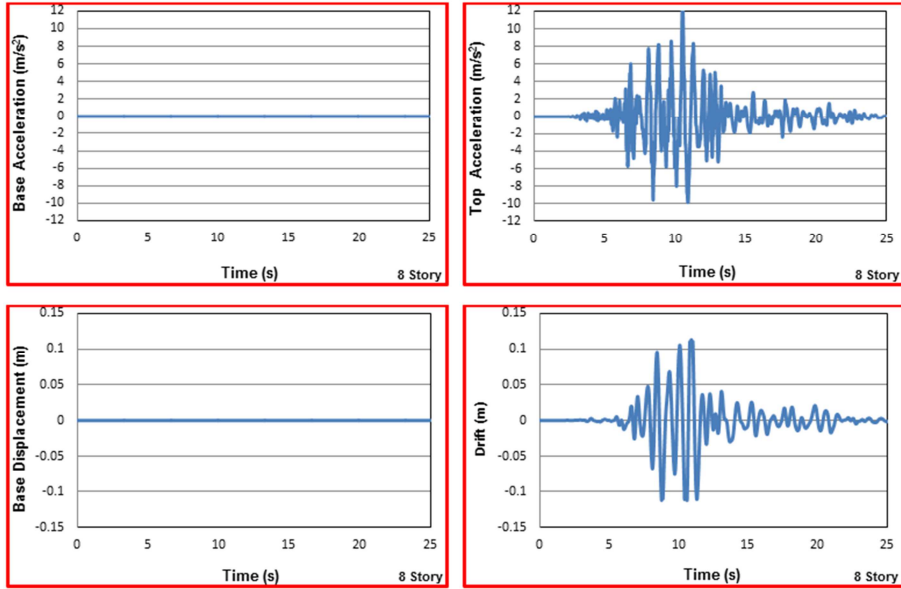


Fig. 7. Base acceleration and acceleration of the highest floor, base displacement and total drift of the 8-story fixed-base building under the Loma Prieta earthquake

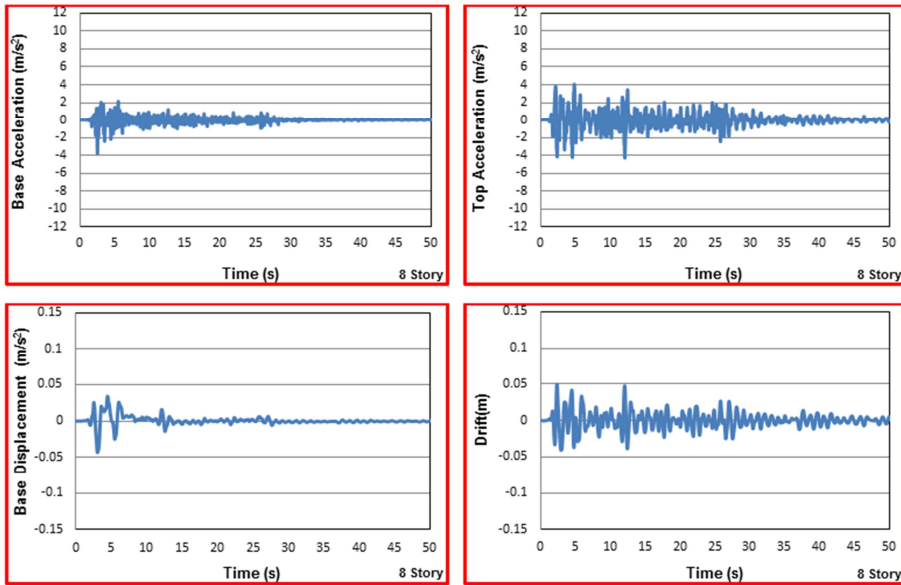


Fig. 8. Base acceleration and acceleration of the highest floor, base displacement and the total drift of the 8-story building with a non-linear seismic isolator with a period of 2 seconds under the Imperial Valley earthquake

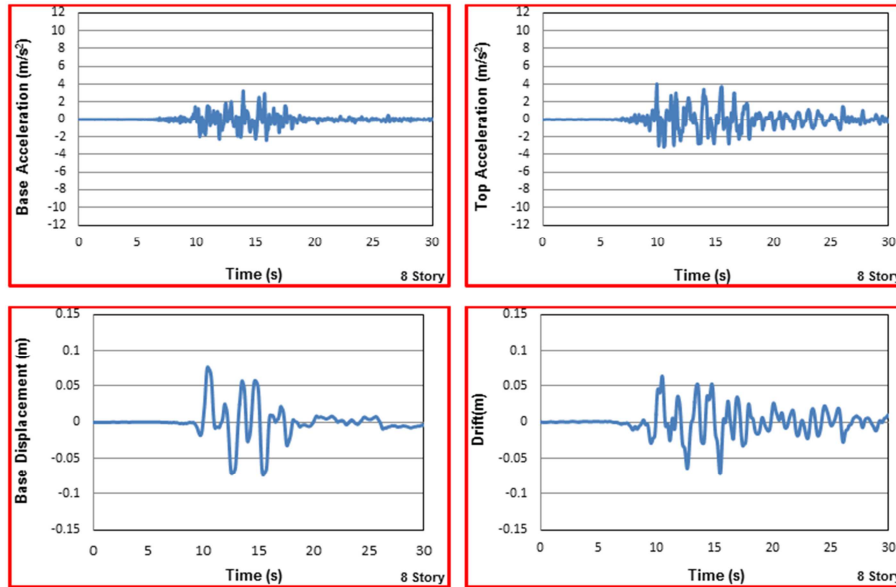


Fig. 9. Base acceleration and acceleration of the highest floor, base displacement and total drift of the 8-story building with a non-linear seismic isolator with a period of 2 seconds under the Kocaeli earthquake

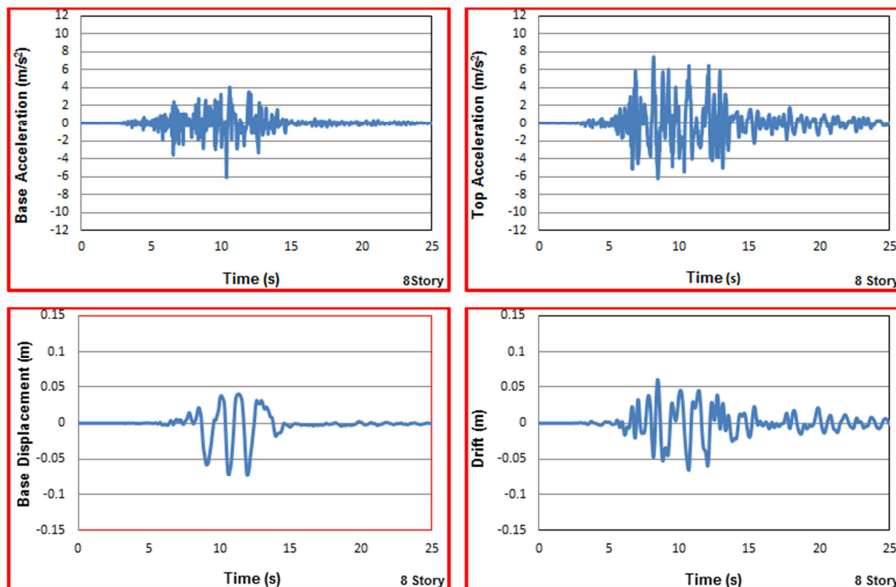


Fig. 10. Base acceleration and acceleration of the highest floor, base displacement and total drift of the 8-story building with a non-linear seismic isolator with a period of 2 seconds under the Loma Prieta earthquake

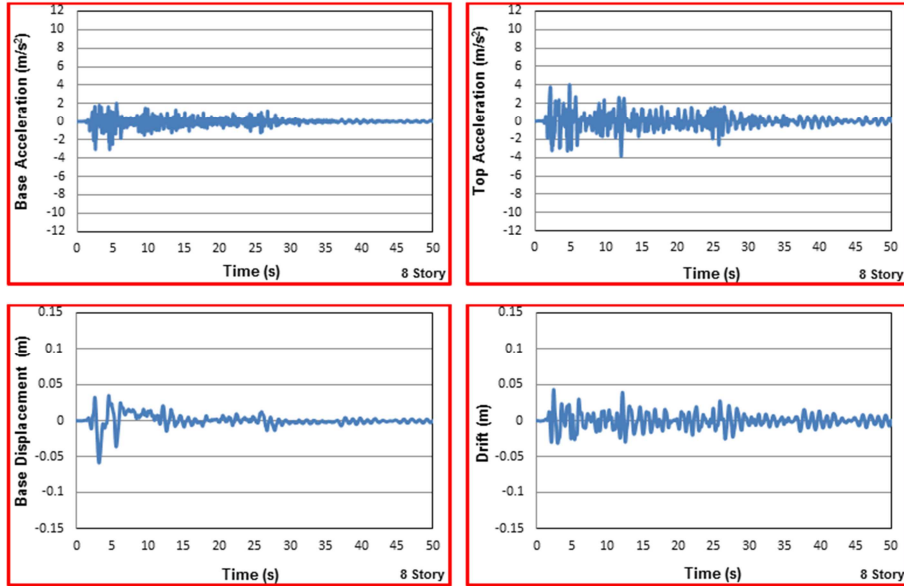


Fig. 11. Base acceleration and acceleration of the highest floor, base displacement and total drift of the 8-story building with a non-linear seismic isolator with a period of 3 seconds under the Imperial Valley earthquake

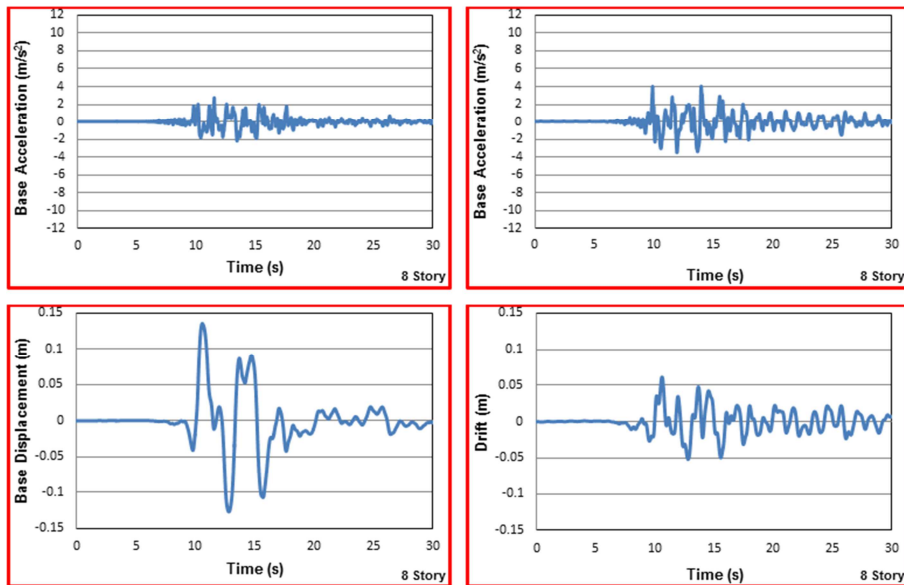


Fig. 12. Base acceleration and acceleration of the highest floor, base displacement and total drift of the 8-story building with a non-linear seismic isolator with a period of 3 seconds under the Kocaeli earthquake

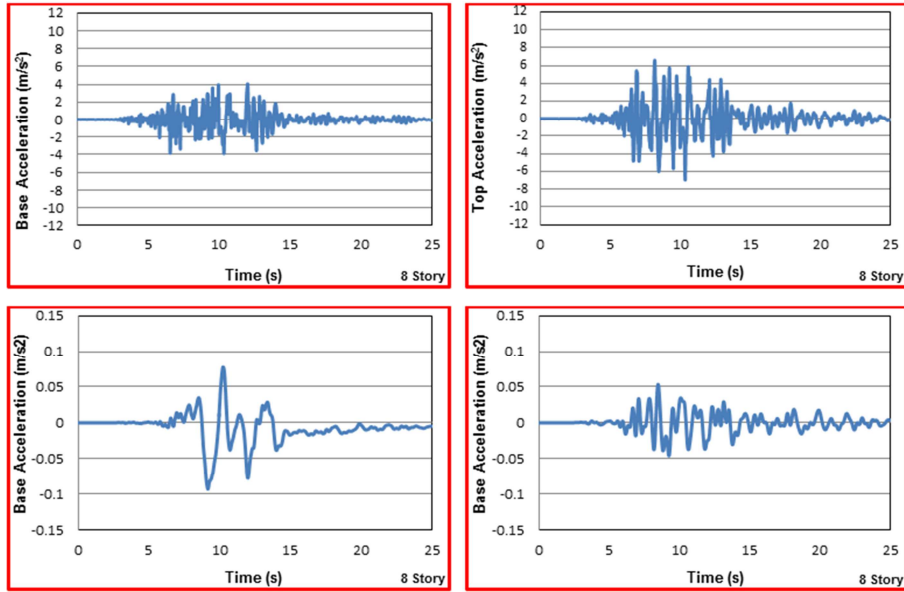


Fig. 13. Base acceleration and acceleration of the highest floor, base displacement and total drift of the 8-story building with a non-linear seismic isolator with a period of 3 seconds under the Loma Prieta earthquake

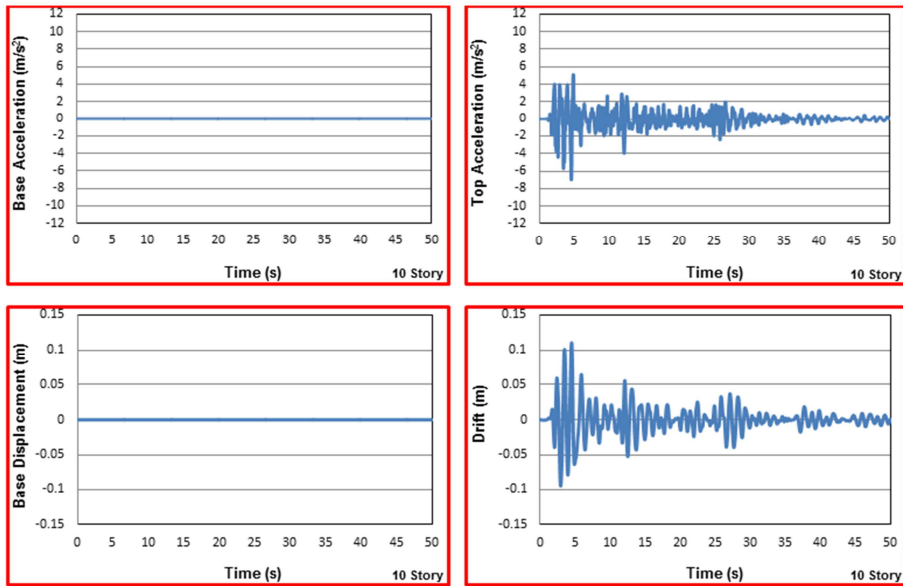


Fig. 14. Base acceleration and acceleration chart of the highest floor, base displacement and total drift of the 10-story fixed-base building under the Imperial Valley earthquake

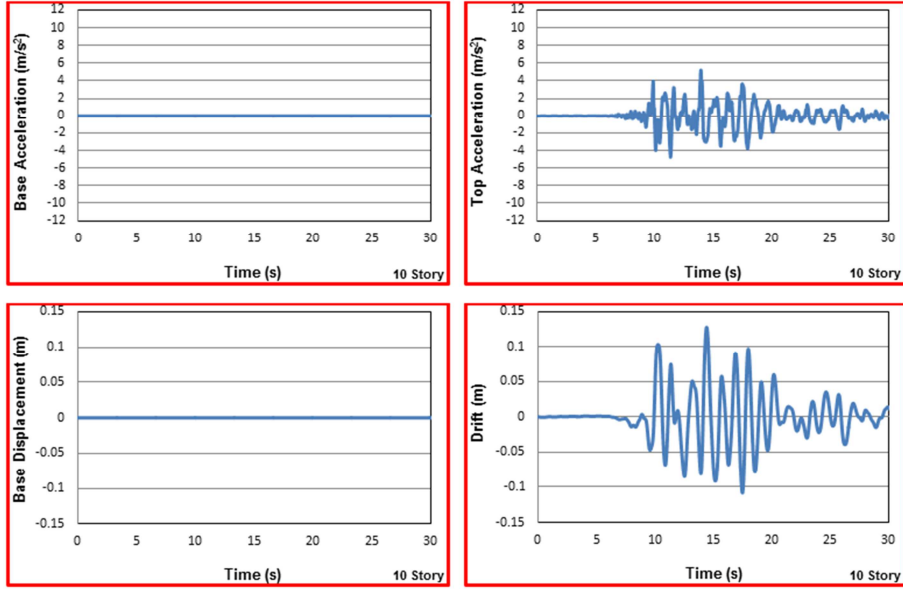


Fig. 15. Base acceleration and acceleration chart of the highest floor, base displacement and total drift of the 10-story fixed-base building under the Kocaeli earthquake

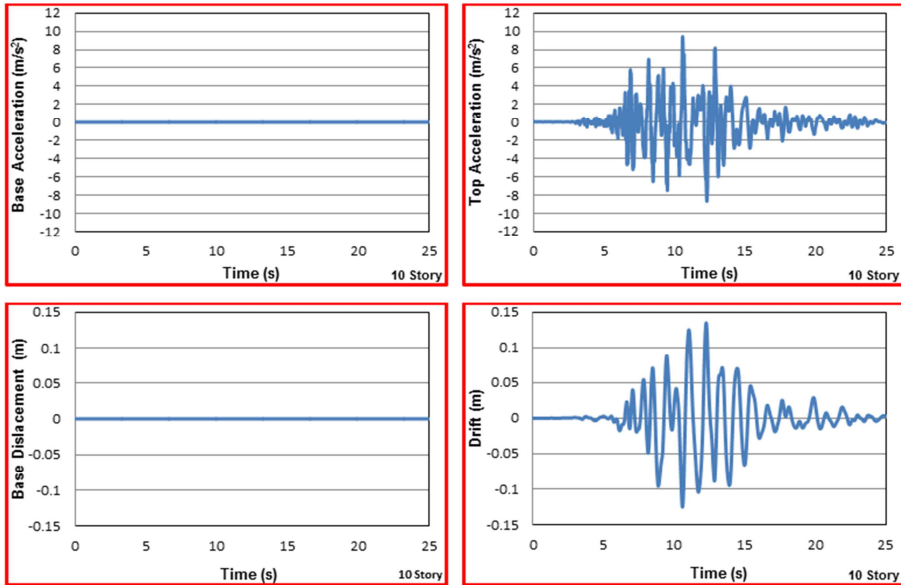


Fig. 16. Base acceleration and acceleration chart of the highest floor, base displacement and total drift of the 10-story fixed-base building under the Loma Prieta earthquake

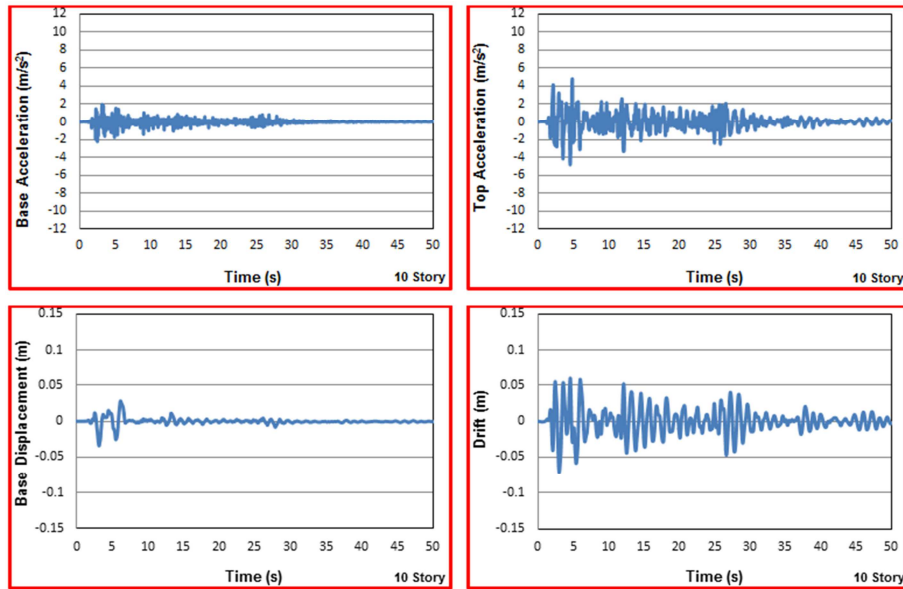


Fig. 17. Base acceleration and acceleration of the highest floor, base displacement and total drift of the 10-story building with a non-linear seismic isolator with a period of 2 seconds under the Imperial Valley earthquake

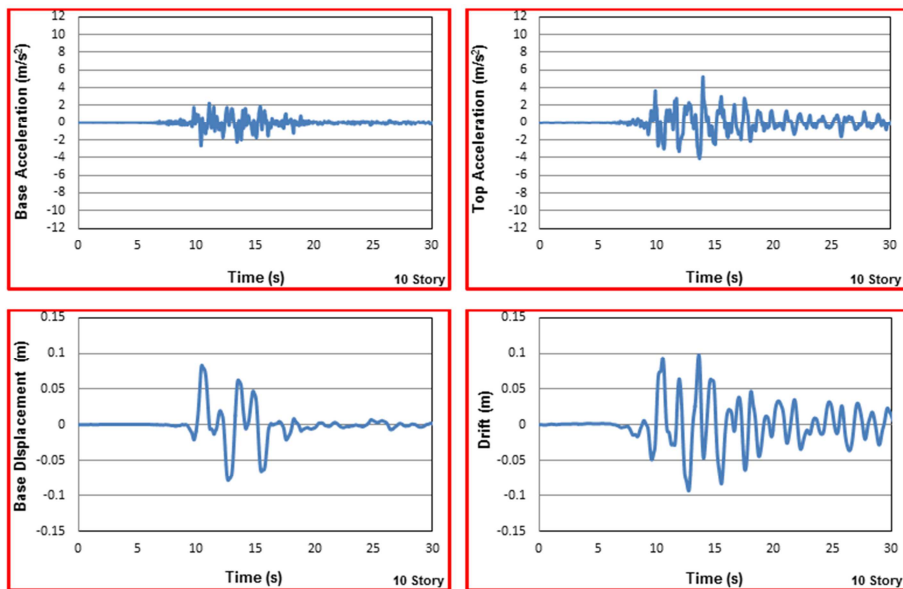


Fig. 18. Base acceleration and acceleration of the highest floor, base displacement and total drift of the 10-story building with a non-linear seismic isolator with a period of 2 seconds under the Kocaeli earthquake

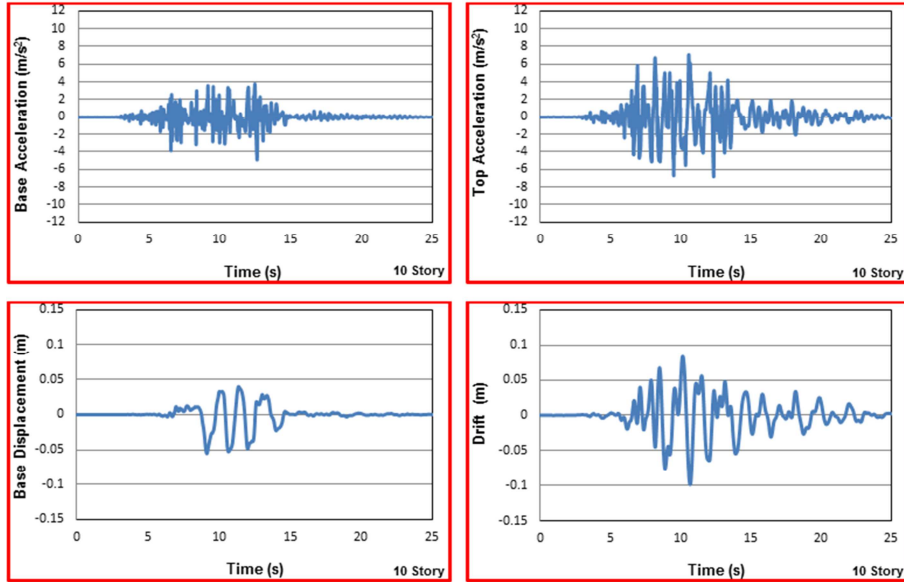


Fig. 19. Base acceleration and acceleration of the highest floor, base displacement and total drift of the 10-story building with a non-linear seismic isolator with a period of 2 seconds under the Loma Prieta earthquake

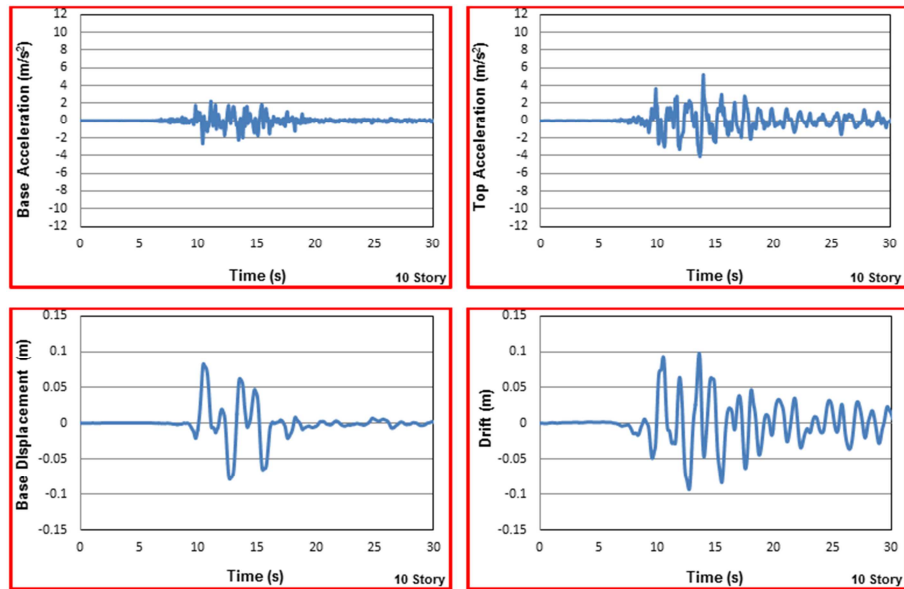


Fig. 20. Base acceleration and acceleration of the highest floor, base displacement and total drift of the 10-story building with a non-linear seismic isolator with a period of 3 seconds under the Imperial Valley earthquake

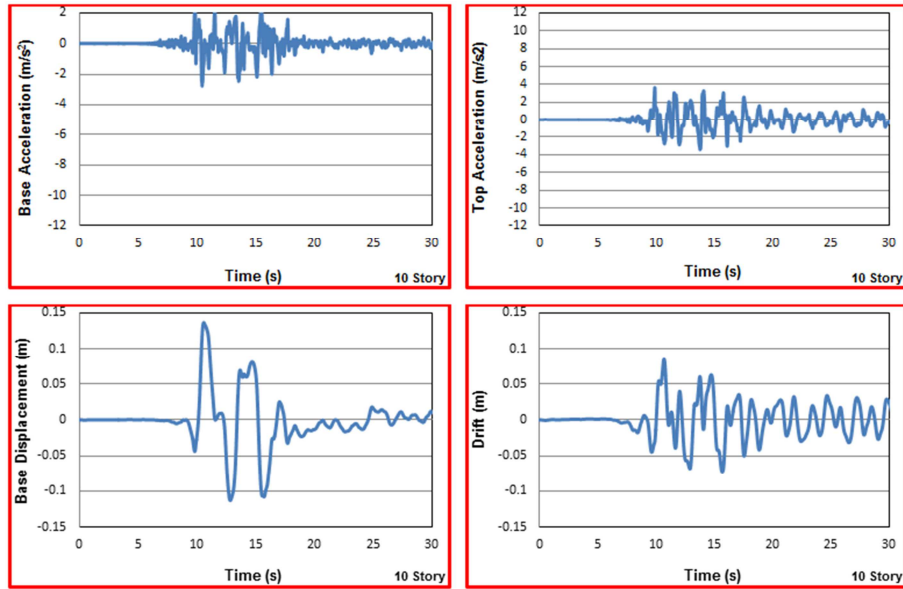


Fig. 21. Base acceleration and acceleration of the highest floor, base displacement and total drift of the 10-story building with a non-linear seismic isolator with a period of 3s under the Kocaeli earthquake

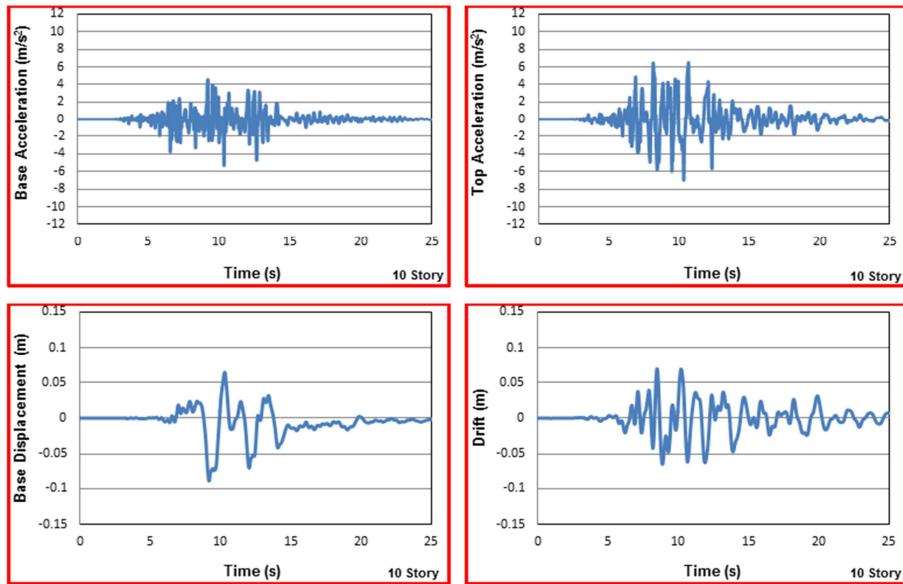


Fig. 22. Base acceleration and acceleration of the highest floor, base displacement and total drift of the 10-story building with a non-linear seismic isolator with a period of 3s under the Loma Prieta earthquake

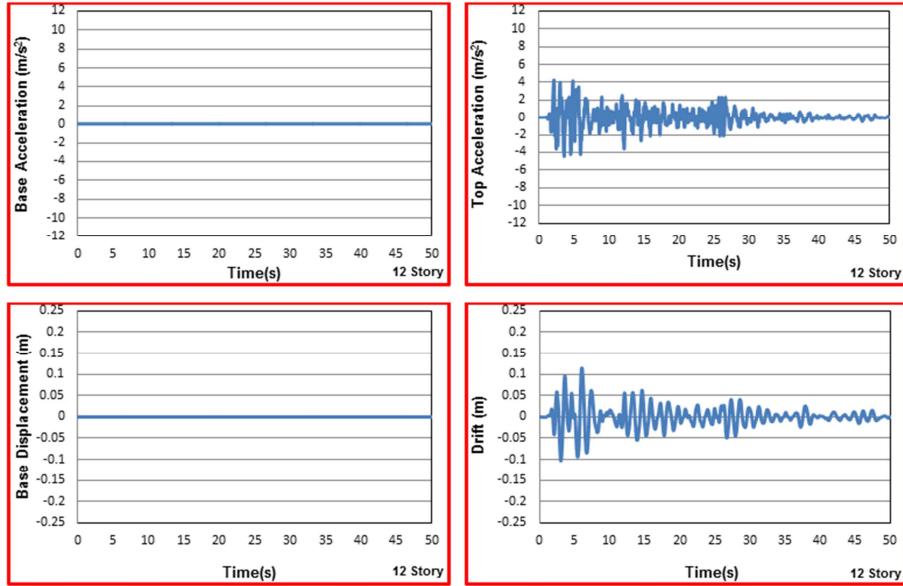


Fig. 23. Base acceleration and acceleration of the highest floor, base displacement and total drift of the 12-story fixed-base building under the Imperial Valley earthquake

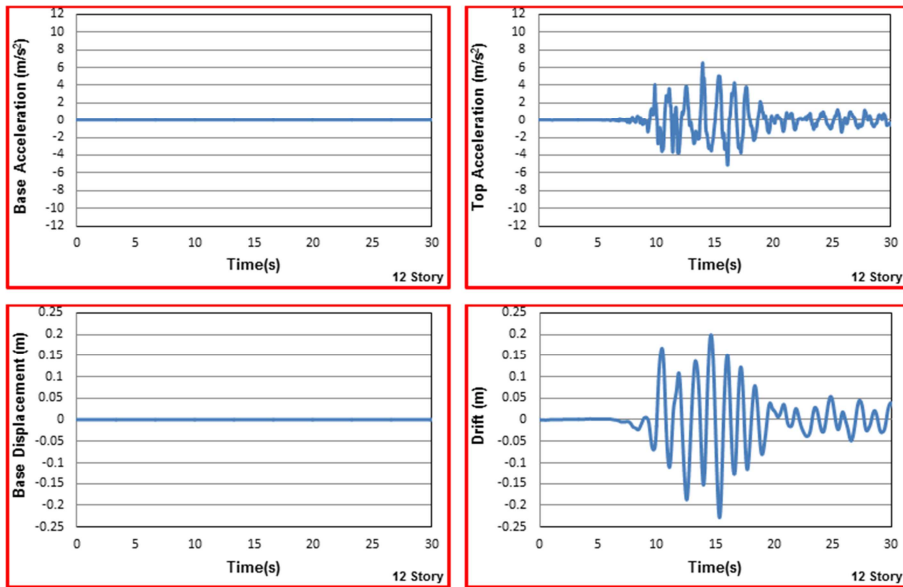


Fig. 24. Base acceleration and acceleration of the highest floor, base displacement and total drift of the 12-story fixed-base building under the Kocaeli earthquake

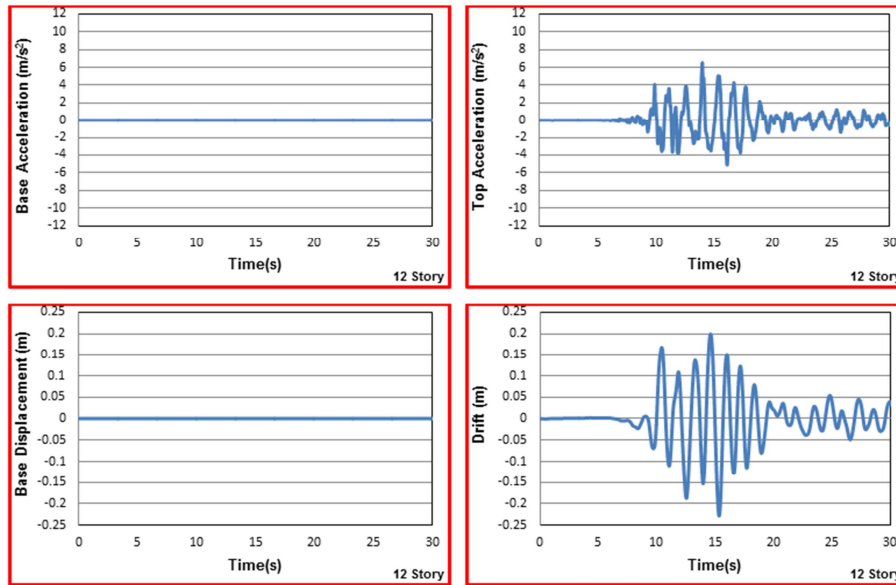


Fig. 25. Base acceleration and acceleration of the highest floor, base displacement and total drift of the 12-story fixed-base building under the Loma Prieta earthquake

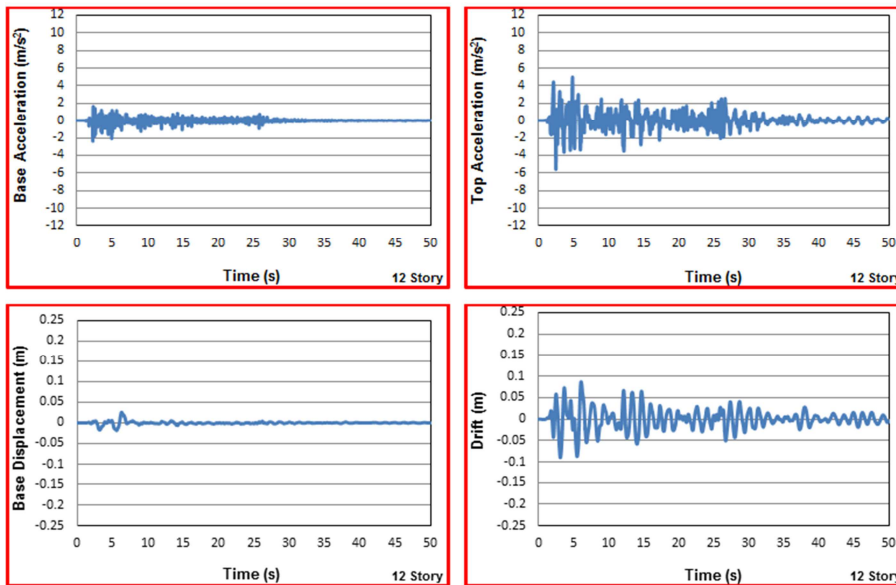


Fig. 26. Base acceleration and acceleration of the highest floor, base displacement and total drift of the 12-story building with a non-linear seismic isolator with a period of 2 seconds under the Imperial Valley earthquake

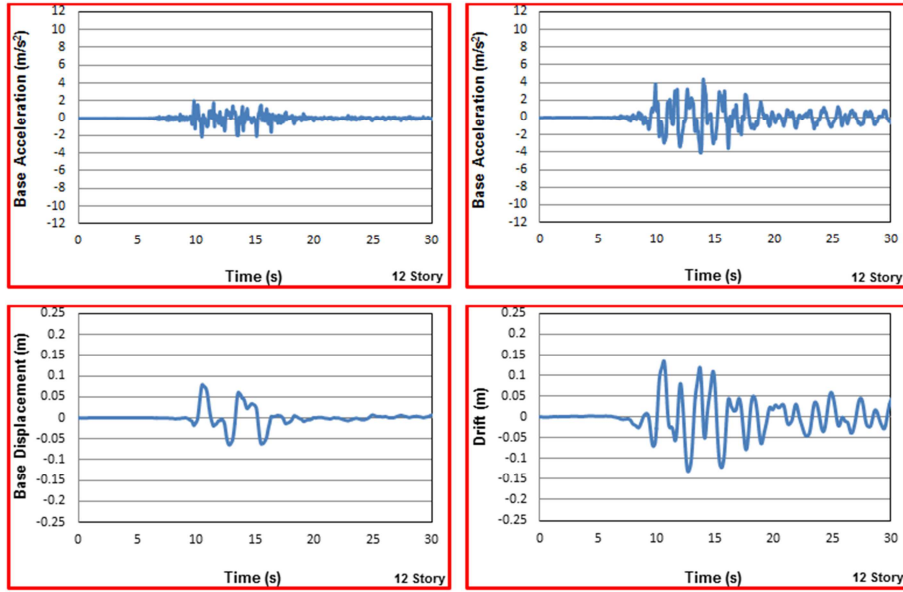


Fig. 27. Base acceleration and acceleration of the highest floor, base displacement and total drift of the 12-story building with a non-linear seismic isolator with a period of 2 seconds under the Kocaeli earthquake

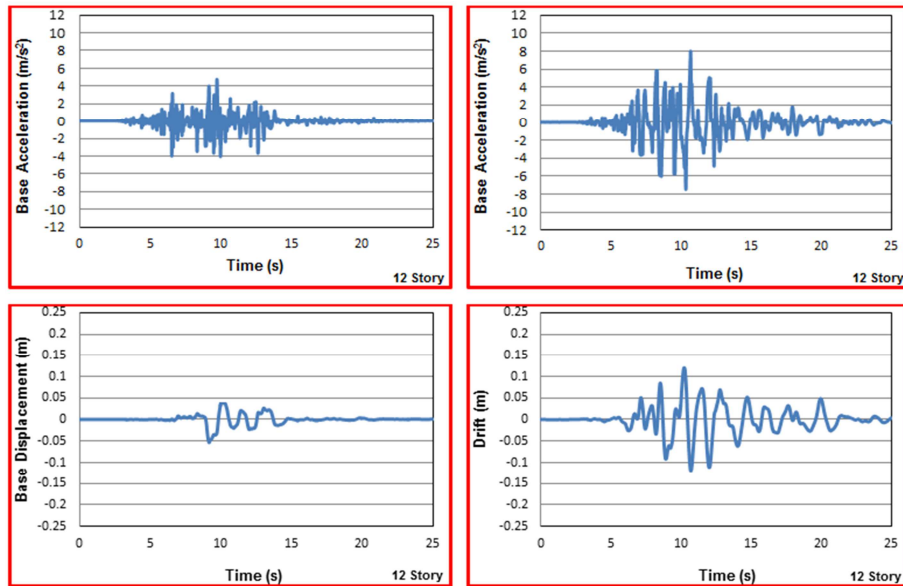


Fig 28. Base acceleration and acceleration of the highest floor, base displacement and total drift of the 12-story building with a non-linear seismic isolator with a period of 2 seconds under the Loma Prieta earthquake

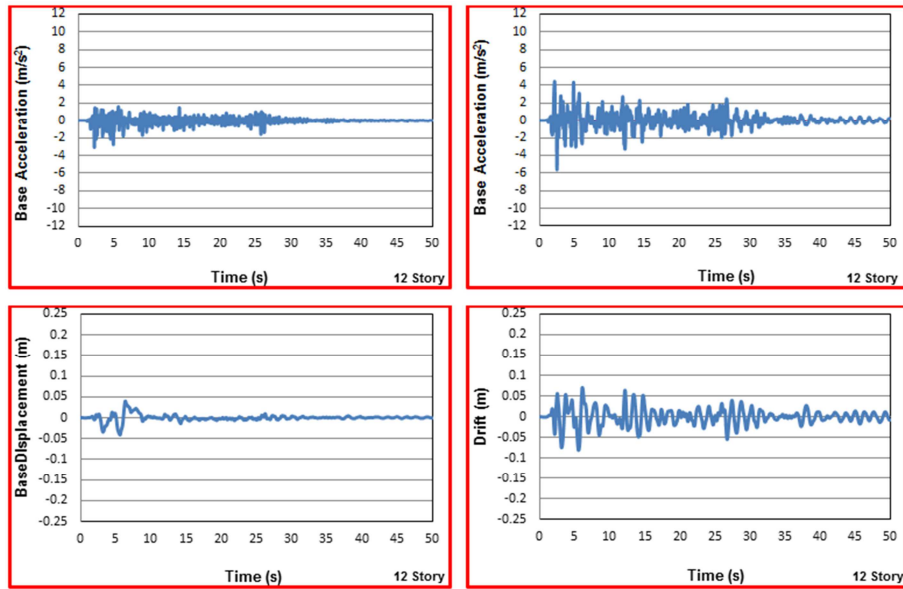


Fig. 29. Base acceleration and acceleration of the highest floor, base displacement and total drift of the 12-story building with a non-linear seismic isolator with a period of 3 seconds under the Imperial Valley earthquake

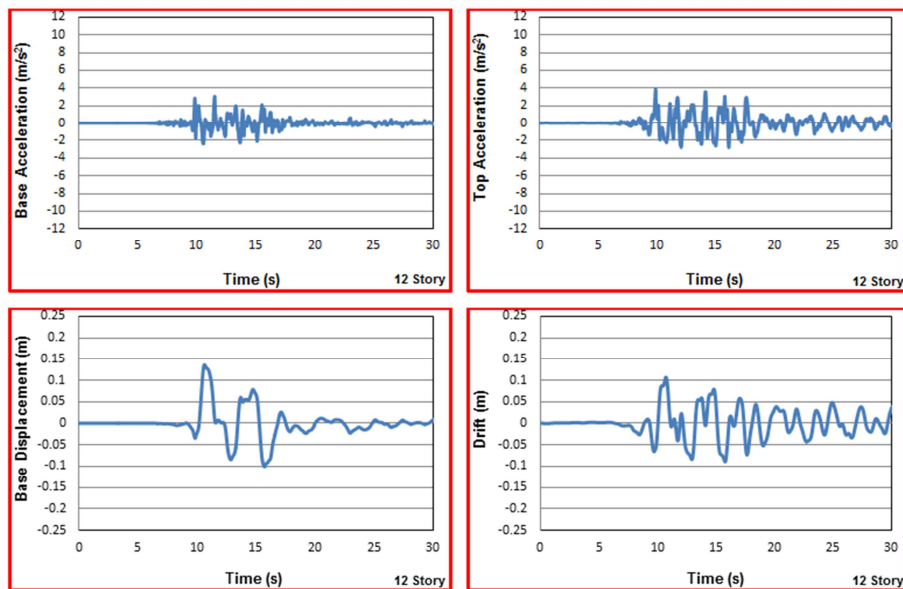


Fig. 30. Base acceleration and acceleration of the highest floor, base displacement and total drift of the 12-story building with a non-linear seismic isolator with a period of 3 seconds under the Kocaeli earthquake

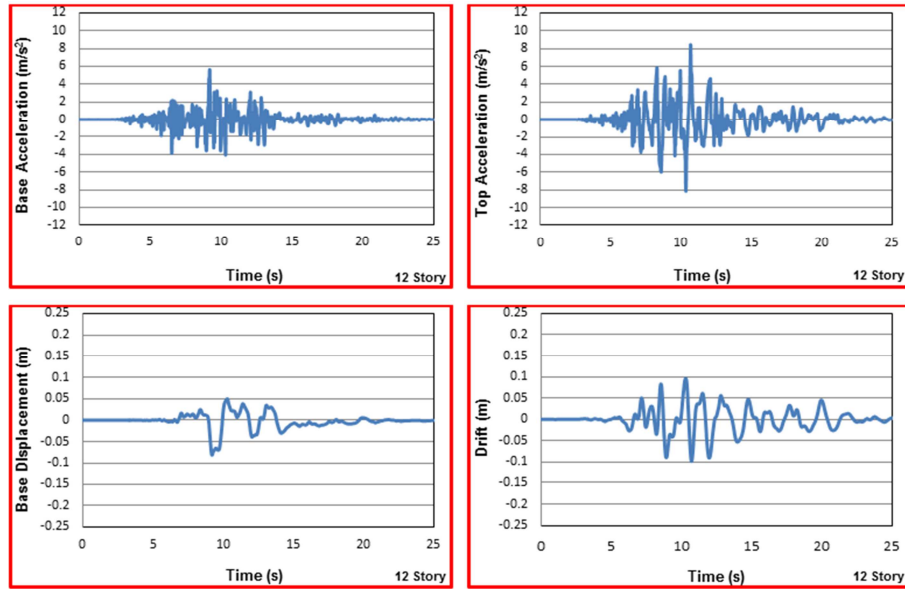


Fig. 31. Base acceleration and acceleration of the highest floor, base displacement and total drift of the 12-story building with a non-linear seismic isolator with a period of 3 seconds under the Loma Prieta earthquake

4.2. Parameter A

Considering the modeling of the buildings and the information on the isolator system, the decrease in the acceleration of the highest floor and total drift in the 8, 10, and 12-story building is as follows:

$$A = \left| \frac{PR (FB) - PR (SI)}{PR (FB)} \right| * 100 \quad (4.1)$$

Where PR (FB) is the largest amount of fixed-base building and PR (SI) is the largest amount of building with seismic isolation system.

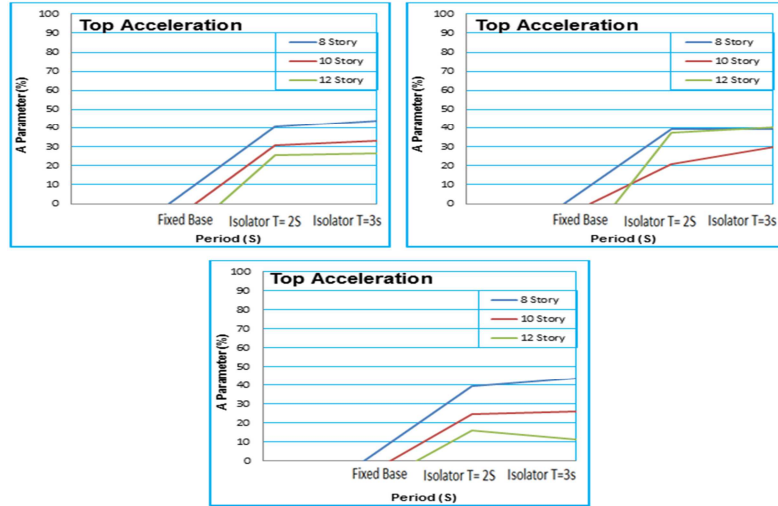


Fig. 32. Decreased acceleration of the highest floor on the 8, 10, and 12-story fixed-base buildings with 2 and 3-second seismic isolator under the different earthquakes; Imperial valley = a, Kocaeli = b, Loma Prieta = c

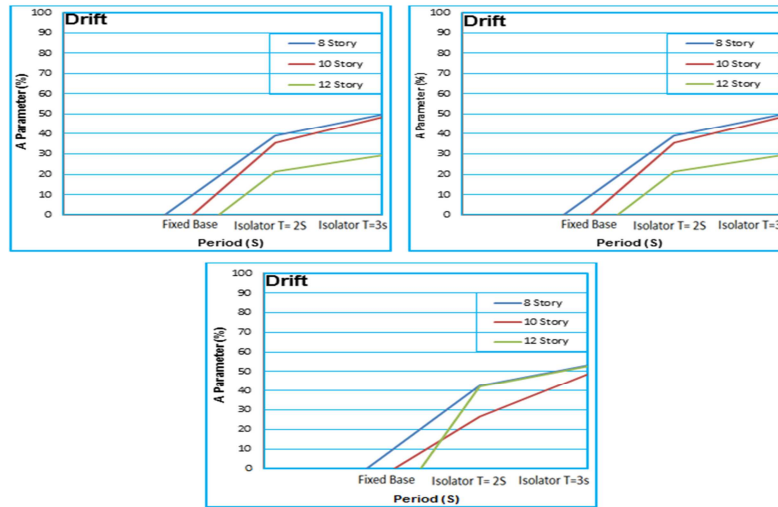


Fig. 33. Drift reduction chart for fixed-base buildings with 8, 10, and 12 floors with 2 and 3-second seismic isolator under the different earthquakes; Imperial valley = a, Kocaeli = b, Loma Prieta = c

4.3. Parameter B

With the increase in the height of the building, how much do the acceleration of the highest floor and the total drift of the building change (the acceleration)

$$B = \left| \frac{PR(8) - PR(10,12)}{PR(8)} \right| * 100 \quad (4.1)$$

Where PR (8) = highest value of 8-story building and PR (10.12) = highest value of 10 and 12-story building.

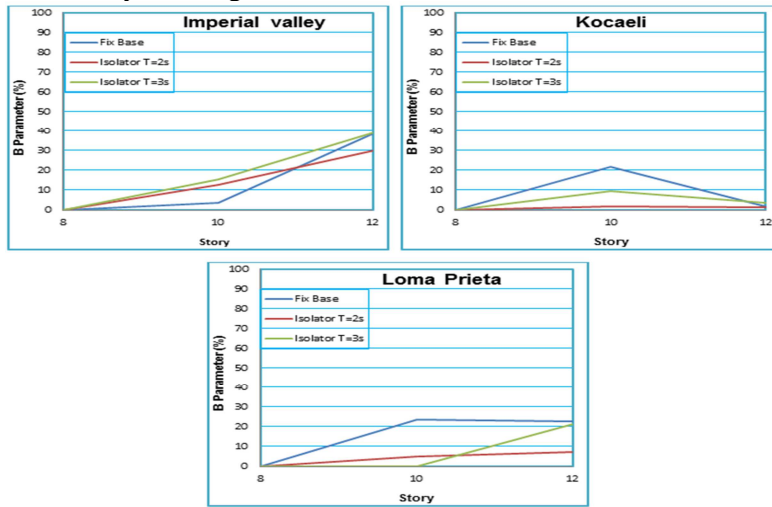


Fig. 34. Acceleration reduction chart of the highest floor of the fixed-base structure with seismic isolator and a period of 2 and 3 seconds considering the increased building height under the Kocaeli, Loma Prieta, and Imperial Valley earthquakes

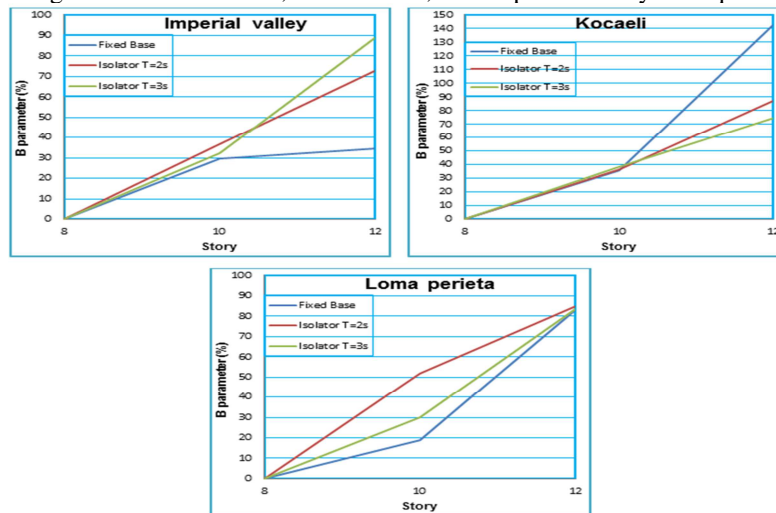


Fig. 35. The total drift increase of the fixed-base building with seismic isolator and a period of 2 and 3 seconds considering the increased building height under the Kocaeli, Loma Prieta, and Imperial Valley earthquakes

5. CONCLUSION

This study used a simple modeling method on a typical high-rise building from the group of regular buildings on the plan.

In this study, three regular isolated buildings were studied in the form of 9 frames, with these buildings all having a fixed base and a seismic isolator of 2 and 3 seconds.

1. The seismic isolation system was used to control the input drift and acceleration of the structure, using a seismic isolation system of 2 and 3 seconds instead of the fixed-base structure. It was observed that in the 8-story building, the value of parameter A in reducing the acceleration to the highest floor was $A_8 = 0-44.71\%$, while $A_{10} = 0-33\%$ for the 10-storey building and $A_{12} = 0-44.45\%$ for the 12-story building. In addition, the value of parameter A in determining the total drift of the building is $A_8 = 0-53.06\%$ for the 8-story building, $A_{10} = 0-48.65\%$ for the 10-storey building, and $A_{12} = 0-53.22\%$ for the 12-story building. The largest change observed in the acceleration of the highest floor and the total drift were associated with the building with a 3-second isolator.
2. Due to the increase in the height of the building from 8 floors to 10 and 12 floors, respectively, the value of parameter B for acceleration of the highest building floor decreased from $B_{8,10} = 0-38.74\%$ to $B_{8,12} = 0-23.76\%$. Furthermore, the building drift increased from $B_{8,10} = 0-51.89\%$ to $B_{8,12} = 0-142\%$, where the highest percentage decrease in acceleration of the highest floor and increased total drift were associated with the fixed-base building as a result of the seismic isolation system reducing the structural response.
3. Due to the high basic period in high-rise structures, the application of seismic isolation systems is decreased. Hence, the use of dampers is recommended to prevent the displacement of buildings over longer periods.

REFERENCES

1. Alhan, C and Sürmeli, M 2011. Shear building representations of seismically isolated buildings. *Bulletin of Earthquake Engineering* **9(5)**, 1643.
2. Baghchesaraei, A and Baghchesaraei, O 2014. The Importance of Infrastructures in the Development of Modern Methods of Construction. *International Journal of Applied Engineering Research* **9(21)**, 11689-11692.
3. Baghchesaraei, O R and Baghchesaraei, A 2015. SPACE DEFINITION IN MODERN AND INNOVATIVE HOUSES. *Indian Journal of Fundamental and Applied Life Science* **5(S2)**, 266-269.
4. Beykzade, M et al. 2019. An Evaluation of Isolated Structures With Seismic Isolators. *Bulletin of the Polytechnic Institute of JASSY, Construction Architecture Section* **65(69)**, 157-168.

5. Beykzade, M and Beykzade, S 2019. Management of Investigating The Effect of Blasting and Impact Load In Various Structures. *Journal of Engineering Science XXVI(3)*. 65-70.
6. Beykzade, M, Baghchesaraei, OR and Heydari Torkamani, M 2018. *Investigation of Liquefaction Dangers By Considering To Liquefaction Susceptibility of The Soil*, 3rd International Energy & Engineering Congress, Gaziantep University, Turkey, October, 18-19.
7. Hwang, JS et al. 1994. Practical analysis of bridges on isolation bearings with bi-linear hysteresis characteristics. *Earthquake Spectra* **10(4)**, 705-727.
8. Hwang, JS et al. 1996. A refined model for base-isolated bridges with bi-linear hysteretic bearings. *Earthquake Spectra* **12(2)**, 245-273.
9. Islam, ABMS et al. 2011. Seismic isolation in buildings to be a practical reality: behavior of structure and installation technique. *Journal of Engineering and Technology Research* **3(4)**, 99-117.
10. Kawashima, K Endo, K Doro, N Sudo, C Nishikawa, I 1992. *Approving test results on four high damping rubber bearings*. proceeding of the 2nd US-Japan Workshop on Earthquake Protective Systems for Bridges Tsukuba, Japan, in December, 7-8, 31-56.
11. Koh, CG and Balendra, T 1989. Seismic response of base isolated buildings including p- Δ effects of isolation bearings. *Earthquake engineering & structural dynamics* **18(4)**, 461-473.
12. Kulkarni, JA and Jangid, RS 2003. Effects of superstructure flexibility on the response of base-isolated structures. *Shock and Vibration* **10(1)**, 1-13.
13. Naeim, F and Kelly, JM 1999. *Design of seismic isolated structures: from theory to practice*. John Wiley & Sons.
14. Nagarajaiah, S et al 1991. Nonlinear dynamic analysis of 3-D-base-isolated structures. *Journal of Structural Engineering* **117(7)**, 2035-2054.
15. Ohtori, Y and Ishida, K 1995. Effect of Experienced Shear Strain Dependency of High Damping Rubber Bearing on Earthquake Response of Isolation Structure. *Journal of Structural and Construction Engineering(Transactions of AIJ)* **60(472)**, 75-84.
16. Tornello, ME and Sarrazin, M 2012. Base-isolated building with high-damping spring system subjected to near fault earthquakes. *Earthquake and Structures* **3(3-4)**, 315-340.
17. Verma, A et al. 2017. Base Isolation System: A Review. *International Journal of Engineering Science Invention* **6(9)**, 43-46.
18. Younis, CJ and Tadjbakhsh, IG 1984. Response of sliding rigid structure to base excitation. *Journal of engineering mechanics* **110(3)**, 417-432.

Editor received the manuscript: 24.04.2020